Universidad Autónoma de Baja California

Facultad de Ingeniería, Arquitectura y Diseño.

Thesis

Production of Si/C Composites by Pyrolysis of Polyurethane and Siloxane for the Fabrication of Lithium-Ion Battery Anodes

Thesis for the degree of:

Bachelor of Engineering in Nanotechnology

Presented By:
Oscar Isaac Lopez Rojas

Thesis Director:
Jassiel Rolando Rodriguez Barreras

Thesis Co-director:
Eunice Vargas Viveros

Ensenada, B.C. April 2025

UNIVERSIDAD AUTONOMA DE BAJA CALIFORNIA
FACULTAD DE INGENIERÍA, ARQUITECTRUA Y DISEÑO
CAMPUS ENSENADA

"Production of Si/C Composites by Pyrolysis of Polyurethane and Siloxane for the Fabrication of Lithium-Ion Battery Anodes"

Thesis

IN ORDER TO FULLFIL THE REQUIREMENTS FOR OBTAINING THE DEGREE OF
NANOTECHNOLOGY ENGINEER

PRESENT

Oscar Isaac Lopez Rojas
361180

To whom the Thesis Committee authorizes the final work, after having carried out a thorough review of it and in accordance with Art. 19 of R.G.E.P.E.P, the professors issue the following evidentiary votes by means of a rubric:

"Por la Realización Plena del Ser"

Jassiel Rolando Rodríguez Barreras, PhD
Director

Eunice Vargas Viveros, PhD
Codirector

Dora Luz Flores Gutiérrez, PhD
Committee member

Sandra Beatriz Aguirre Vega, PhD
Committee member

Enrique Efren García Guerrero, PhD
Committee member

ABSTRACT

The growing environmental impact of plastic waste, particularly polyurethane (PU), which is challenging to recycle due to its thermosetting properties, has prompted the development of sustainable recycling methods. In this study, pyrolysis was utilized to decompose PU into carbon, which was then combined with polydimethylsiloxane (PDMS) to synthesize a silicon-carbon (Si/C) composite. This approach not only addresses the issue of PU waste but also creates a material that combines the high lithium storage capacity of silicon with the structural stability of carbon. The composite, composed of 25 wt% PDMS and 75 wt% pyrolyzed PU, was successfully synthesized and used to fabricate an electrode for lithium-ion batteries. Material characterization techniques, including XRD, SEM, and TGA, confirmed a uniform distribution of silicon particles, low crystallinity, and high thermal stability, with a residual mass of 42% after pyrolysis. Electrochemical performance was evaluated through cyclic voltammetry (CV), galvanostatic cycling, and diffusion coefficient calculations. The results revealed well-balanced charge storage mechanisms, with B values close to 0.7, suggesting a combination of diffusion-controlled and capacitive processes. The Li^+ diffusion coefficients were significantly improved in comparison to pure silicon, and the capacitive contributions were substantial, enabling rapid charge-discharge capabilities. Although the composite does not reach the performance levels of high-end commercial batteries, its straightforward synthesis, low cost, and sustainable approach make it a promising candidate for practical applications in next-generation energy storage systems. This work demonstrates the potential of recycling PU waste into functional materials for advanced battery technologies.

RESUMEN

El creciente impacto ambiental de los desechos plásticos, particularmente el poliuretano (PU), que es difícil de reciclar debido a sus propiedades termoestables, ha impulsado el desarrollo de métodos de reciclaje sostenibles. En este estudio, se utilizó la pirólisis para descomponer el PU en carbono, que luego se combinó con polidimetilsiloxano (PDMS) para sintetizar un compuesto de silicio-carbono (Si/C). Este enfoque no solo aborda el problema de los desechos de PU, sino que también crea un material que combina la alta capacidad de almacenamiento de litio del silicio con la estabilidad estructural del carbono. El compuesto, compuesto por 25% en peso de PDMS y 75% en peso de PU, se sintetizó con éxito y se utilizó para fabricar un electrodo para baterías de iones de litio. Las técnicas de caracterización de materiales, incluyendo XRD, SEM y TGA, confirmaron una distribución homogénea de partículas de silicio, baja cristalinidad y excelente estabilidad térmica, con una masa residual del 42% después de la pirólisis. El rendimiento electroquímico se evaluó mediante voltametría cíclica (CV), ciclos galvanostáticos y cálculos del coeficiente de difusión. Los resultados revelaron mecanismos de almacenamiento de carga equilibrados, con valores b cercanos a 0.7, lo que indica una mezcla de procesos controlados por difusión y capacitivos. Los coeficientes de difusión de Li^+ mejoraron significativamente en comparación con el silicio puro, y las contribuciones capacitivas fueron sustanciales, permitiendo capacidades de carga-descarga rápidas. Aunque el compuesto no alcanza los niveles de rendimiento de las baterías comerciales de alta gama, su simplicidad, rentabilidad y síntesis sostenible lo convierten en un candidato prometedor para aplicaciones prácticas en sistemas de almacenamiento de energía de próxima generación. Este trabajo demuestra el potencial de reciclar desechos de PU en materiales funcionales para tecnologías avanzadas de baterías

ACKNOWLEDGMENTS

I would like to express my gratitude to Universidad Autónoma de Baja California, through Facultad de Ingeniería, Arquitectura y Diseño, for providing me with the education and the opportunity to develop in various fields, not only within the University but also beyond. I am thankful to the CICESE institution and Dr. Jassiel Rolando Rodriiguez Barreras for their guidance, advice, and the time they dedicated to this thesis, as well as for sharing their knowledge with me.

I would also like to thank the thesis committee for their valuable evaluation and feedback, which were fundamental in the development and improvement of this work I am grateful to all my undergraduate professors for imparting their knowledge, time, and patience, which were crucial in completing my academic training.

I am deeply thankful to my parents for their constant support throughout my studies and especially during the completion of this thesis. To my sister, I am grateful for her insights and experience in project execution and decision-making.

TABLE OF CONTENTS:

LIST OF FIGURES:

LIST OF TABLES:

1.- INTRODUCTION

Plastic waste effects have become increasingly apparent in recent years, impacting both health and the environment. While most research on this issue has focused on the marine environment, studies indicate that plastic waste in landfills and poorly managed recycling systems also pose significant risks. These risks stem primarily from the chemicals used in synthesizing plastics such as Bisphenol A, phthalates, and flame retardants, which are known to be harmful to both animals and humans.

The actual impact of plastics on health remains largely uncertain, as the mechanisms by which these chemicals affect living organisms are not fully understood. The most common pathway of exposure is through ingestion. Once ingested, the chemicals in plastics can bioaccumulate through the food chain, potentially exposing entire ecosystems to their harmful effects.

To further understand the problematics of recycling plastics, it is important to know the difference between thermoplastics and thermosets. Thermoplastics are a type of polymer, that can be easily heated until melted or softened, making them easy to mold and recycle. Therefore, these polymers are generally produced in one step and then converted into the required article at a subsequent stage.

On the other hand, thermosetting plastics have superior properties like high thermal stability, rigidity, dimensional stability, and resistance to creep or deformation under load. This is due to their strong 3D covalent bond network, which provides better thermal stability than thermoplastics. Therefore, these materials cannot be recycled or reformed under high temperatures.

Two important factors influence and determine the viability of thermoplastics recycling. These are the prices of the recycled polymer compared with the virgin polymer and the cost of recycling compared with alternative forms of acceptable disposal. The primary methods of waste disposal are landfill and incineration. Costs of landfills vary considerably among regions according to the underlying geology and land-use patterns and can influence the viability of recycling as an alternative disposal method. For example, in Japan, landfill excavation is expensive due to the hard nature of the

underlying volcanic bedrock; while in the Netherlands, it is costly because of permeability from the sea. The price of virgin plastic is determined by the price of oil, which is the principal feedstock for plastic production. As the quality of the recovered plastic is usually lower than the virgin plastic, the price of virgin plastic is the maximum price for recovered plastic.

Among the various types of plastics, polyurethane (PU) stands out due to its widespread use and the significant challenges it presents in terms of recycling. PU has a wide range of high-performance properties; it represents a major class of polymers with applications in medical, automotive, and industrial fields. Due to the large number of starting materials, PU exhibits various organic chemical behaviors. As a result, PU stands for a product range or plastics-industry segment rather than a single polymer resin. A simple way of classifying different PU is by their density and the rigidity. The variety of PU types ranges from flexible/rigid foams and thermoplastic elastomers to adhesives.

Rigid polyurethane foams (PUF) constitute an important group of PUF due to their wide applications as a heat insulator in refrigeration, buildings, and construction materials. Their low thermal conductivity results from a bulk density of 30–35 kg/m³ and a closed-cell structure filled with insulating gas. In this research, we will be focusing on soft PUF due to its widespread use and significant contribution to plastic waste. Soft PUFs have a virtually completely open-cell structure with typical densities of 20-45 kg/m^3. Thus, soft PUFs are not effective as insulators and are instead commonly used in seats and furniture due to their softness and light weight.

Due to the wide range of varieties of PU's, it makes it very difficult to develop a cost-efficient recycling method. Recycling routes for PU can be divided into three types: "*mechanical recycling"*, "*chemical recycling"*, and "*energy recovery"*. Mechanical recycling involves grinding, compression molding, and adhesive pressing of PU waste; chemical recycling breaks specific bonds to recover valuable materials; and energy recovery refers to incineration, decomposition, and combustion of PU waste. For our investigation, we will be using the "Energy recovery" method, or more specifically, the "Thermochemical recycling" method to use the PU as raw material for the preparation of carbon-based materials, and then, the fabrication of electrodes.

Pyrolysis is a well-known recycling process for PU wastes; it utilizes a heated, oxygen-free environment to pyrolyze plastics into gasses and a mixture of monomers. The temperatures used in this process are typically 400 °C - 800 °C. The process produces gas, oil, and charcoal — the latter being a fine powder containing carbon black, ash, and inorganic residues, which is our material of interest. Other important parameters for a pyrolytic process are heating rate, reaction time, and pressure, which significantly influence the material's morphology, composition, and structural properties. The heating rate affects the decomposition of precursors and the rate at which volatile compounds are released, potentially leading to differences in porosity or particle size. Reaction time determines the extent of material conversion and the formation of the desired phases, while pressure can alter the reaction kinetics, influencing the final density and crystallinity of the synthesized material. These factors are crucial in optimizing the pyrolysis process to obtain materials with tailored properties for specific applications.

The pyrolysis products will be used to elaborate an anode for a Lithium-ion battery (LIB). An anode is the negative electrode during discharge and the positive pole during charging in a secondary cell. The basic requirements for a LIB anode material are that the material should have minimal volume expansion and stress during the charge/discharge process, high electronic conductivity, chemical and mechanical stability under a wide range of operation temperature, and low specific surface area for optimal performance and safety.

The most commonly used anode materials are carbonaceous, as they possess the advantages of low cost, excellent reversible capacity, and long cycle performance. Carbonaceous materials have a large number of variations in crystallinity, chemical composition, and microtexture depending on their preparation, processing, precursor, thermal, and chemical activation treatments. Graphitic carbons are characterized by layers of hexagonally arranged carbon atoms in planar graphene layers where the lithium ions can be stored during charge and released during a discharge of the cycle. However, compared with other alternative anode materials, the theoretical capacity of graphite is low to accomplish the minimum requirement from batteries with high energy density.

An alternative material for an anode is Silicon. Si has drawn attention as a promising anode material since the discovery of its superior theoretical Li storage capacity in the 1980s, significantly higher than that of graphite. The packing density in Li-Si alloys is very close to or slightly higher than that in pure Li metal. Si also possesses a low discharge potential, rich natural abundance, and environmental benignity. However, the realization of Si as a LIB anode has been held back because of its large specific volume changes during lithiation and delithiation.

To address the limitations of both graphite and silicon as anode materials, our study proposes the synthesis of a composite material by combining graphite with silicon. By integrating silicon into the graphite matrix, we aim to leverage the high capacity of silicon while mitigating its volume expansion through the structural stability provided by a carbonaceous material. This composite aims to improve battery performance by enhancing energy density and cycling stability. The charcoal produced from the pyrolysis process will be utilized in the fabrication of this innovative anode material, potentially offering a sustainable and efficient solution for plastic waste recycling and energy storage applications.

2.- JUSTIFICATION

This study aims to address the significant environmental issue of plastic waste, particularly focusing on PU, which is challenging to recycle. By exploring the use of recycled PU in battery electrodes, this research not only seeks to reduce plastic waste but also to enhance battery technology. The study employs thermochemical recycling, specifically pyrolysis, to break down PU and repurpose its components. This innovative strategy aims to reduce landfill waste while advancing sustainable and efficient energy storage technologies.

3.- THEORETICAL FRAMEWORK

Brief introduction

The theoretical framework of this research provides a comprehensive understanding of the scientific and technological context underpinning the study, focusing on the escalating environmental and health impacts of plastic waste and the need for sustainable solutions. This research addresses the utilization of PU waste, a significant and challenging category of plastics, through pyrolysis, and a thermal decomposition process. The goal is to transform PU waste into valuable materials for fabricating anodes for lithium-ion batteries (LIBs). The framework begins with an overview of the environmental and health implications of plastic waste, followed by a detailed examination of the chemical properties and recycling challenges associated with thermoplastics and thermosets, particularly PU.

The framework then explores the principles and parameters of the pyrolysis process, highlighting its potential to convert PU waste into useful products such as charcoal. This charcoal, characterized by its high carbon content, is investigated as a precursor for anode materials in LIBs. The discussion extends to the properties and performance requirements of anode materials, focusing on the limitations of conventional graphite and the advantages and challenges of silicon. Finally, the framework reviews the synthesis and benefits of composite materials combining graphite and silicon to enhance anode performance. By integrating insights from previous studies and current advancements, the theoretical framework establishes a solid foundation for the proposed research, emphasizing its relevance and potential impact on sustainable waste management and energy storage technology.

3.1 Plastic waste issues

Plastic debris has emerged as a pervasive global pollutant in recent years, contaminating terrestrial, marine, and freshwater environments worldwide. The very qualities that make plastic so useful—its low cost, durability, lightweight nature, and hydrophobic properties—also contribute to its environmental harm. The low cost of plastic leads to mass production and predominantly single-use applications. Despite

the growing global production and consumption of plastic products, waste management systems remain insufficient in many regions. Consequently, an estimated 31.9 million metric tons of plastic enter the natural environment annually (Jambeck et al., 2015). Once in the environment, plastic's durability allows it to persist for centuries or even millennia, while its lightweight nature facilitates long-distance transport by wind and water currents. Furthermore, its hydrophobic properties cause plastic to absorb environmental contaminants, which can alter the transport and bioavailability of chemicals within ecosystems and affect wildlife health (Geyer et al., 2017).

In the environment, macroplastics (>5 mm) are broken down into smaller microplastics (less than 5 mm) through exposure to sunlight and/or wave action. Plastic debris is found in agricultural fields, soil, roadways, urban stormwater runoff, freshwater systems, and the open ocean. Terrestrial and aquatic wildlife encounter these micro- and macroplastics in virtually every habitat on Earth. Aquatic organisms at all trophic levels from primary producers like algae, to primary consumers such as zooplankton, and top predators like whales, fish, turtles, seabirds, and seals, have been documented ingesting or interacting with plastic (Schell et al., 2020).

Within terrestrial environments, there are comparatively fewer primary research articles documenting similar interactions. However, given the extent of plastic pollution and its propensity to spread, it is likely that terrestrial wildlife are equally affected. For example, microplastic ingestion has been observed in terrestrial birds, along with reports of anthropogenic debris incorporated into their nests. Concerns about the impacts of plastic on both aquatic and terrestrial wildlife are frequently raised in scientific literature, policy documents, and media reports (Schell et al., 2020).

3.2 Environmental and health impacts of plastic waste

The pathways and distribution of microplastics in the environment are complex, with their presence in the food chain raising significant environmental and human health concerns. Numerous studies have highlighted the intricate nature of microplastic contamination and its consequences within the food chain. The widespread presence

of microplastics in soil and their uptake by plants and animals indicate a potential route of human exposure through agricultural consumption (Sharma & Vidyarthi, 2024).

Microplastics pose a significant threat to human health, with links to liver, digestive, and reproductive toxicity, as well as an increased risk of cancer. Table 1 illustrates some pathways of microplastics in the food chain and their potential health impacts. Their pervasiveness throughout ecosystems highlights the urgency of implementing robust mitigation and regulatory strategies. Effective waste management practices play a crucial role in minimizing plastic waste entering the environment, thereby reducing microplastic generation (Sharma & Vidyarthi, 2024).

Table 1. *Environmental and health microplastics pathways concerns (Sharma & Vidyarthi, 2024).*

Aspect	**Description**	**Environmental concerns**	**Health concerns**
Ingestion by Animals	Consuming contaminated feed, water, or environments	Accumulation in tissues and organs of animals, potential entry into the human food chain	Potential health risk due to ingestion of microplastics present in meat, dairy, and other animal products
Soil-to-plant uptake	Absorption of microplastics by plants	Uptake by plants grown in contaminated soil, potential human consumption	Uncertainty about health impacts from ingestion of crops contaminated with microplastics

3.3 Polyurethanes (PU)

Developed by Professor Otto Bayer in 1937, polyurethane (PU) is a synthetic polymer that entered industrial production after World War II. This highly versatile material is integral to everyday life, from rigid foam insulation in construction to automotive seat cushions and elastomers in medical devices. By adjusting raw materials and formulations, PU products can be tailored into elastomers, thermoplastics, and thermosetting resins. However, traditional PU production relies on petrochemicals, raising environmental and health concerns (Waleed & Fiser, 2019).

Rigid PU foams are widely used as versatile and energy-efficient materials. They offer significant energy cost reductions while enhancing the comfort and efficiency of commercial and residential appliances. Proven effective as insulation, these foams are used in window, wall, and roof insulation, as well as in air and door sealants. Flexible PUFs, developed over the past four decades, are essential in cushioning, packaging, and safety applications and come in slabstock, molded, and integral skin forms (Waleed & Fiser, 2019).

Slabstock foam is designed for lower-density applications, primarily in cushioning and packaging. Density affects not only product cost but also comfort levels. Molded foam typically occupies a mid-range density for applications requiring some load-bearing capacity. The distinction between molded foam and integral skin foam, however, can be somewhat blurred, as skin formation is an inherent characteristic of molded PU systems. Integral skin foams, a type of molded foam, are produced by injection into closed, vented, or open molds. These foams feature a high-density outer skin and a softer, lower-density core (Waleed & Fiser, 2019).

Polyurethane (PU) has become one of the most important polymers in the plastics industry in recent years, ranking as the sixth most commonly used worldwide, with an annual production of approximately 18 million tons. Numerous studies and experimental investigations have explored the utilization of PU waste. The non-biodegradable components of PU waste include petroleum-derived hydrocarbons that pose toxicity and flammability hazards. Currently, three methods are used for PU waste disposal: landfilling, incineration, and recycling. However, due to the difficulty of decomposing PU in landfills and its unfavorable physical and chemical characteristics for this technique, landfilling is not a viable option (Sani et al., 2024).

Polyurethane (PU) can be recycled through various methods, including chemical recycling, which breaks down the material into its constituent chemicals, and mechanical recycling, which reuses the material in its polymeric form. Among these approaches, chemical processes (such as alcoholysis, hydrolysis, and fractionation), thermochemical processes (such as pyrolysis and gasification), and energy recovery methods (such as thermal degradation and municipal waste combustion) are most

commonly employed for obtaining monomers and recovering energy (Sani et al., 2024).

3.4 Pyrolysis

Pyrolysis is a thermochemical process involving the thermal decomposition of polymers in an oxygen-free environment at high temperatures. This process generates various products, including hydrocarbon distillates and non-condensable gases. The resulting pyrolysis oil is inherently unstable, both chemically and thermally, and can undergo further reactions such as esterification, oxidation, and polymerization. Several factors influence the pyrolysis process, including heating rates, temperature, catalyst type, residence time, and feedstock composition. The main products from PU pyrolysis include monomers and various organic compounds, such as acidic, heterocyclic, and oxygenated carbon-based molecules (Sani et al., 2024).

Pyrolysis, one of several thermochemical methods including hydrothermal liquefaction, thermal desorption, incineration, and gasification, is particularly effective for energy recovery and produces a non-hazardous end product. During pyrolysis, mass loss begins around 250 °C to 300 °C, with approximately 80% of the mass lost in this range. The remaining 20% of mass loss occurs at 500 °C. The primary goal of PU pyrolysis is to maximize the production of char while minimizing the yield of oil products. While PU foam pyrolysis can occur in two temperature ranges, 25 °C to 400 °C and above 400 °C, the majority of the degradation takes place between 200 °C and 400 °C typically under an inert atmosphere such as nitrogen to prevent oxidation. (Sani et al., 2024).

3.5 Lithium-Ion battery anodes

Lithium-ion batteries (LIBs), which hold a 63% share of the global battery market, are widely used in electronic devices, electric vehicles, and renewable energy storage systems. LIBs are primarily composed of an electrolyte, separator, cathode, and anode. The electrolyte acts as the medium for Li^+ ion transport during electrochemical reactions. Positioned between the cathode and anode, the separator, a polymeric barrier film, prevents short circuits while ensuring efficient Li^+ ion transfer within the electrolyte. The cathode facilitates lithium insertion/extraction, while the anode allows

reversible intercalation and deintercalation of Li^+ ions, enabling current flow through an external circuit. Anode materials typically offer a higher capacity compared to cathode materials (Yang et al., 2024).

Nowadays, commercial LIB anode materials primarily rely on graphite due to its low operating potential, abundant reserves, and electrochemical stability. However, graphite's isotropic structure limits its theoretical capacity to 372 mAh/g, which is insufficient for the high energy density and fast charging demands of applications like electric vehicles (Yang et al., 2024). As a result, hard carbon (HC) has gained prominence as a next-generation anode material for alkali metal-ion batteries. Derived from various precursors, including petroleum pitch, coal tar pitch, polymers, and biomass, HC is a largely non-graphitizable form of carbon. Its disordered structure provides numerous active sites for ion storage, leading to high capacity and cycling stability (Saju et al., 2024).

Due to their excellent overall performance, HC anodes are gaining considerable interest as a replacement for graphite anodes in LIBs. The disordered microstructure of HCs offers numerous pathways for Li^+ ion incorporation, facilitating efficient intercalation and deintercalation. Additionally, HC anodes demonstrate enhanced cycling performance and fast-charging capabilities, making them promising for high-performance LIB applications. These distinct properties have driven the development of HC materials for next-generation LIBs with increased energy storage. Optimizing HC anode design during cycling and enhancing overall rate performance remain key research areas (Saju et al., 2024).

3.6 Silicon as anode material

Given the abundant reserves and low cost of graphite and its precursors, along with straightforward processing methods, graphite holds a dominant position in the commercial Li-ion battery market. However, its relatively low energy density has driven the search for alternative anode materials with higher specific capacity, such as silicon (Si). Electronic devices, particularly digital products, require compact energy sources to minimize space requirements, highlighting the importance of high volumetric energy

density. Silicon's ability to alloy with multiple lithium ions allows it to achieve a much higher volumetric energy density than graphite (Zhao et al., 2024).

Silicon microparticles, being semiconductors, exhibit low electronic conductivity, display Li^+ ion diffusion coefficients ranging from 10^{-14} to 10^{-13} cm^2/s, and possess a high specific capacity (4200 mAh/g). However, not all lithium ions are reversible during cycling, limiting efficiency. Furthermore, Si nanoparticles have a large specific surface area, and upon exposure to the electrolyte, high-resistance by-products readily form on the surface, consuming active materials and diminishing the actual capacity. Volume expansion during lithiation leads to particle cracking, exposing fresh surfaces to further electrolyte reactions (Zhao et al., 2024).

At room temperature, the initial lithium insertion process in crystalline Si involves a phase transition from single crystal to polycrystalline, eventually becoming amorphous. When charging under high-temperature conditions, Si undergoes a series of phase changes corresponding to different voltage plateaus. There is a direct correlation between the degree of volume expansion and the amount of lithium embedded in the silicon anode. When Si transforms into Li44Si, the volume expansion of the alloyed Si anode results in pulverization and detachment of active materials from the electrode, further causing a break in the conductive network and loss of capacity. As a result, lithium-ion batteries with Si-based anodes tend to exhibit lower initial coulombic efficiency (Zhao et al., 2024).

3.7 Carbon and silicon composites

To minimize the expansion rate of the material while increasing the coulombic efficiency, Si-C hybrid anodes have become the most practical solution and have started to be used in commercial batteries. Although carbon has a lower theoretical capacity than silicon, it offers advantages such as lower cost, better mechanical strength, and excellent electrical conductivity. Therefore, Si-C hybrid materials can help alleviate material fragmentation caused by the volume expansion of Si and enhance the transmission ability of electrons and ions (Zhao et al., 2024).

The key to preparing Si/C composites lies in distributing Si particles uniformly on the surface of carbon, especially for nano-sized Si particles, which are highly prone to agglomeration. Agglomeration of nano-Si particles may lead to uneven current distribution, mechanical failure, and reduced electrochemical performance (Li et al., 2024). Much research has been conducted to overcome the drawbacks of using Si anodes, including silicon/carbon compositing and converting Si to nanopillars, nanotubes, and nanowires. However, many synthesis techniques for nano-Si anodes are sensitive and energy-intensive, limiting their scalability. Si/C composite is being considered extensively because of its excellent operability, while carbon offers high electrical conductivity and cycle stability (Fafure et al., 2024).

The production of Si/C anodes began with Wilson et. al. in 1995 when they embedded 11% of “atomic silicon in pre-graphitic carbon” (Wilson et al., 1995). Since then, numerous studies have been conducted, improving the performance of Si/C anodes. Despite progress, challenges persist, including the high cost of raw materials, complex synthesis processes, and environmental concerns related to some components. Therefore, a key strategy in achieving environmentally friendly and low-cost raw materials is the extraction of Si/C anodes from eco-friendly, naturally occurring, and recyclable materials (Fafure et al., 2024).

4.- BACKGROUND

4.1 Historical context

Since the 21st century, the energy crisis and environmental pollution resulting from the excessive use and burning of traditional energy sources have driven a global shift towards renewable energy development. Consequently, the storage and conversion of energy have become the focus of current scientific research. Lithium-ion batteries have gained significant attention for their high operating voltage, low self-discharge, stable discharge voltage, high energy density, excellent cycling performance, no memory effect, wide operating temperature range, long working life, and environmentally friendly nature. They are widely used in electronic devices, vehicles, medical treatment, communication, and aerospace applications (Zhao, Zuo, et al., 2024).

The anode, a crucial component of LIBs, significantly influences their electrochemical performance. Currently, graphite, a crystalline form of carbon, is the primary negative electrode material for commercial LIBs due to its abundant availability, low cost, mature processing technology, and safety. When it is used as a negative electrode material, graphite demonstrates good electrical conductivity, high reversible lithium storage capacity, and low charge/discharge potential. Although graphite is more advantageous than other negative electrodes, there was considerable resistance when it first emerged as an anode material. Its development history is shown in Figure 1. In the 2020s, researchers have continued to explore graphite anode materials, focusing on increasing energy density, reducing cost, and minimizing environmental impact (Zhao, Zuo, et al., 2024).

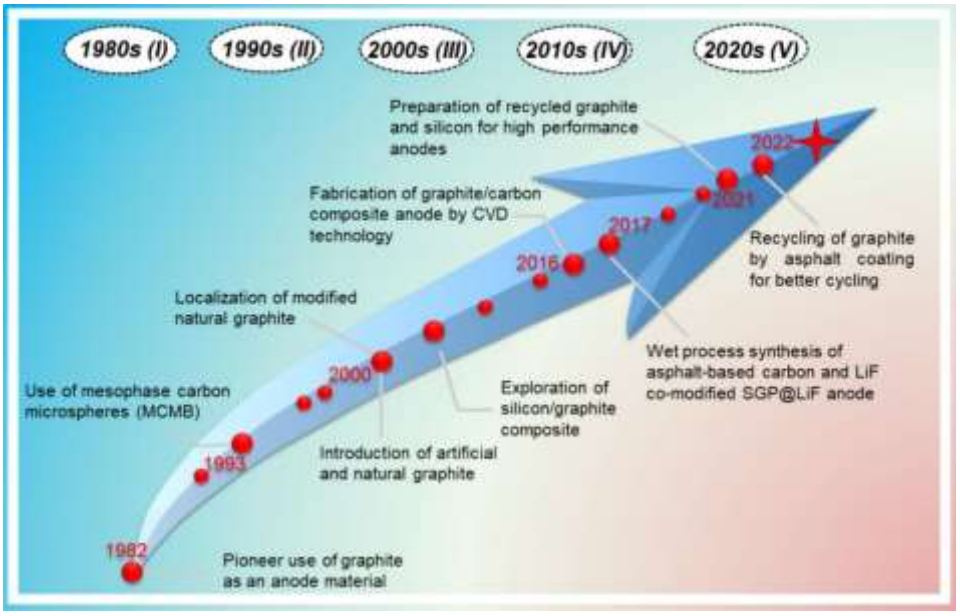

Figure. 1 *History and development of graphite negative electrode materials (Zhao, Zuo, et al., 2024).*

4.2 Disadvantages of graphite anodes

Anodes in many commercial-grade lithium-ion batteries are made of graphitic carbon. Graphite is best described as a stack of hexagonally bonded carbon sheets held together by Van der Waals forces. The forces between any two carbons in the same sheet (which share sp^2 hybridized bonds) are much stronger than those between any two adjacent sheets. It is due to this disparity in forces that Li^+ ions can be inserted between the planes of graphite. This process, known as insertion or intercalation, is the mechanism through which graphitic anodes can store Li. During intercalation, Li ions occupy interstitial sites between adjacent graphene layers in graphite. Once inserted, a Li^+ prevents other ions from binding directly adjacent interstitial sites. This restriction limits lithium binding to every second carbon hexagon, resulting in a maximum stoichiometry of LiC_6. This directly affects the energy storage density of graphite in LIBs (De Las Casas & Li, 2012). Figure 2 illustrates this process, showing (a) lithium insertion at every second carbon hexagon, and (b) lithium residing between the graphite layers.

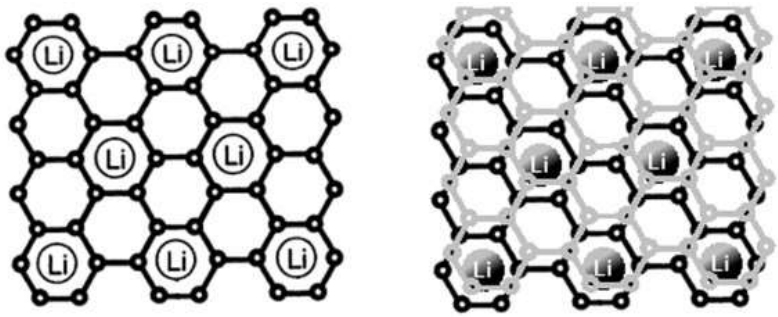

Figure. 2 *Scheme of Lithium intercalation in graphite. (a) Lithium is inserted in every 2nd carbon hexagon and (b) between the graphite layers (De Las Casas & Li, 2012.*

4.3 Research of silicon/graphite composite electrodes

The development of Si/G composite marks a milestone in the advancement of LIB technology. Silicon exhibits an exceptionally high theoretical specific capacity of 4200 mAh/g, greatly surpassing the 371 mAh/g of conventional graphite. However, silicon experiences significant volume expansion during charging and discharging, leading to structural rupture and capacity loss. To address this, researchers have developed Si/Gr composites that combine silicon’s high energy density with the electrical conductivity and mechanical stability of graphite. This combination not only alleviates the swelling problem of Si but also significantly enhances the overall performance of the battery (Zhao, Zuo, et al., 2024).

4.4 Research of silicon/graphene composite electrodes

Recent advancements in Si/graphene composites have shown their potential to overcome the limitations of Si anodes for lithium-ion batteries. Incorporating graphene as a conductive buffer matrix enhances the mechanical stability of the composite, effectively accommodating the volumetric expansion of silicon during cycling. Additionally, graphene's large surface area and mechanical flexibility prevent the agglomeration of Si nanoparticles, which is crucial for maintaining the integrity of the electrode. When configured in a core–shell structure with a carbon coating, the design minimizes direct contact between silicon and the electrolyte, thereby reducing SEI instability and improving cycle life (Zhou & Liu, 2024).

The 3D porous framework of graphene also plays a significant role in the electrochemical properties of these composites. This architecture helps buffer mechanical stress, improves charge transport, and enhances ion diffusion, ultimately leading to superior rate capability. Such synergistic benefits make Si/graphene composites a top candidate for enhancing the longevity and performance of next-generation lithium-ion batteries, offering a balanced approach to capacity retention and cycle stability (Zhou & Liu, 2024).

4.5 Research of silicon/carbon nanotubes composite electrodes

Carbon nanotubes (CNTs) are essential in enhancing the functionality of Si-based anodes in LIBs. Their high electrical conductivity and exceptional mechanical strength make them suitable as both conductive frameworks and structural reinforcements. Available in single-walled, double-walled, and multi-walled forms, CNTs can accommodate silicon's significant volume expansion (~400%) during the lithiation/delithiation process. This accommodation improves structural stability, mitigates electrode pulverization, and stabilizes the solid electrolyte interface (SEI), resulting in enhanced cycling performance (Kang et al., 2024).

One of the key advantages of CNTs is their versatility in binder-free electrode configurations, where they provide sufficient adhesion and conductivity without the need for additional binding agents. Scalable production methods for CNTs—including chemical vapor deposition (CVD), arc discharge, and flame synthesis—support their potential for commercial application. Incorporating CNTs into Si/C composites simplifies electrode fabrication and boosts performance, addressing challenges like low conductivity and capacity fading associated with silicon-based anodes (Kang et al., 2024).

However, CNT-enhanced Si/C composites do have certain limitations. Despite manufacturing advancements, the high production cost of CNTs remains a major obstacle to widespread adoption. Additionally, challenges such as potential CNT aggregation and uneven distribution within the composite can reduce their effectiveness. Ongoing research aims to optimize composite design, improve CNT dispersion, and reduce fabrication costs to ensure commercial viability for next-generation LIBs. (Kang et al., 2024).

5.- HYPOTHESIS

Polyurethane and polydimethylsiloxane are successfully pyrolyzed and resulting in the formation of a silicon-carbon (Si/C) composite with efficient electrochemical activity for lithium storage in lithium-ion battery anodes.

6.- GENERAL OBJECTIVE

Synthesize a Silicon-carbon Si/C composite from PU and PMDS through pyrolysis to fabricate electrodes for the assembly of a half-cell lithium-ion battery.

6.1.- Specific objectives

- Synthesize Si/C composite material through pyrolysis of PU and PDMS.
- Prepare homogeneous slurries using Si/C composites, Polyvinylidene fluoride (PVDF), N-Methyl-2-pyrrolidone (NMP), and Super P carbon.
- Fabricate Si/C composite electrodes exhibiting low interfacial resistance and high electrochemical stability.
- Assemble a half-cell lithium-ion battery using Si/C composite-based electrodes.
- Evaluate the Si/C electrodes' performance and kinetic behavior using cyclic voltammetry, determining diffusion coefficients, *b*-values, and capacitive/intercalation contributions

7.- MATERIALS AND METHODS

The experiments, including the synthesis, fabrication, design, assembly, characterization and testing of the materials and electrodes, were conducted at Centro de Investigación Científica y de Educación Superior de Ensenada (CICESE) and Centro de Graduados e Investigación en Química (CGIQ). These activities were made possible through the collaboration and guidance of Jassiel Rodríguez, PhD, whose expertise and resources were instrumental in facilitating the experimental processes necessary for this project.

7.1.1 Materials

The materials listed in Table 2 were used as precursors for the pyrolysis, components of the active paste, and for coating onto the copper foil current collector.

Table 2. *Reagents and Materials Used in the Synthesis and Fabrication of Electrodes*

REAGENT NAME	DESCRIPTION	SUPPLIER/ORIGIN	USE IN THE PROJECT
Recycled PU	Recycled PU plastic	Recycling source	Raw material for synthesizing the Si/C composite.
PDMS	High-purity silicone polymer	MLsolar	Precursor for composite material formation.
Carbon SP	Conductive carbon	Sigma-Aldrich	Enhances the electrode's conductivity.
NMP	Solvent	Sigma-Aldrich	Dissolves PVDF to prepare the active paste.
PVDF	Binder	Sigma-Aldrich	Binds the components of the electrode paste.
Copper foil/roll	Thin copper sheet	MTI Corporation	Acts as the current collector for the electrode.

7.1.2 Synthesis of Si-based nanocomposite

The pyrolysis of PU with PDMS was carried out to form a carbon/This process was designed to combine the structural stability of carbon with the high capacity of silicon for lithium-ion storage applications. The pyrolysis was conducted in a tubular furnace, using a sealed reactor to encapsulate the precursors. This setup ensured uniform thermal decomposition and prevented contamination from the external environment. The process was performed under an argon atmosphere, which was essential to prevent oxidation during high-temperature heating, promoting carbon structure formation from PU and converting PDMS into silicon-based nanocomposites. The combination of PU and PDMS via pyrolysis provided an efficient route to obtain a material with high storage capacity and good cycling stability, both essential for enhancing battery performance.

7.2 Electrode and battery fabrication

The preparation of the electrodes involved several steps to ensure the fabrication of high-quality components for the half-cell. First, the active paste was prepared by mixing PVDF, NMP, Carbon SP, and the synthesized Si/C composite. These materials were thoroughly combined to form a homogeneous slurry, which served as the electrode material.

Next, the prepared paste was evenly spread onto a copper foil, creating a thin film approximately 100 micrometers thick. The coated foil was then dried for 24 hours to allow complete evaporation of the solvent, resulting in a uniform composite layer.

After drying, the copper foil with the composite layer was punched into small circular electrodes using a specialized puncher. Electrodes were carefully weighed, and the most uniform samples were selected to ensure consistency in electrochemical performance.

The half-cell assembly was conducted in a controlled environment inside a glove box under an Ar-atmosphere to prevent contamination from moisture and air. Each cell included a working electrode, a separator, an electrolyte, and a lithium metal counter

electrode. The components were pressed to ensure a proper seal, enhancing both the structural integrity and the electrochemical performance of the cell.

Photographic documentation was performed throughout the process, including steps such as paste preparation, electrode formation, electrolyte injection, sealing, and electrochemical testing, as illustrated in Figure 3.

Figure. 3 *Lithium-Ion battery assembly and testing workflow. i) Raw material, ii) Si/C electrodes, iii) Dripping of electrolyte into the battery case, iv) Hydraulic press for battery sealing, v) Voltage test, vi) Cyclic Voltametric analysis.*

7.3 Material characterization

7.3.1 Scanning electron microscopy (SEM)

Scanning Electron Microscopy (SEM) is a characterization technique that uses a focused beam of electrons to scan the surface of a sample, producing high-resolution images that reveal detailed information about the surface topography and composition. The SEM operates by detecting secondary electrons emitted from the sample when it is bombarded with an electron beam, providing insights into morphology and structural features.

In this study, SEM was employed to identify agglomerations and analyze the distribution of silicon (Si) particles on carbon (C). The instrument was operated at an accelerating voltage of 11.0 kV, which influenced image resolution and depth of field.

7.3.2 X-Ray diffraction (XRD)

X-Ray Diffraction (XRD) is a powerful analytical technique used to determine the crystallographic structure, crystallinity, and phase composition of materials. It operates by directing X-rays at a sample and detecting the angles and intensities of diffracted beams, which reflect the atomic arrangement within the material. This information is used to infer the arrangement of atoms within the crystal lattice.

As illustrated in Figure 4, XRD operates based on Bragg's Law, which relates the wavelength of the X-rays and the diffraction angle to the distance between atomic planes in a crystal. When Bragg's Law conditions are satisfied, constructive interference generates distinct diffraction peaks, enabling structural analysis.

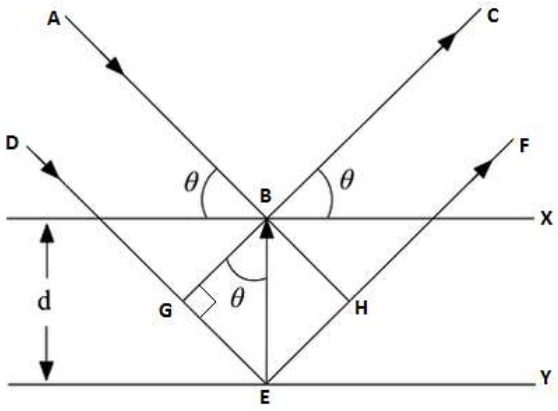

fig: Bragg's Law

Figure. 4 *Representation of Bragg's law. (Malla, s. f.)*

In this study, XRD was utilized to verify the crystallinity of the material and identify possible phases present in the composite. Measurements were conducted using a step size of 0.0153° over a 2θ range of 15° to 80°, allowing high-resolution structural evaluation.

7.3.3 Thermogravimetric analysis (TGA)

Thermogravimetric Analysis (TGA) is a technique used to measure the change in mass of a material as a function of temperature or time. This method provides insights into thermal stability, decomposition behavior, and material composition. During controlled heating, weight loss is recorded to assess material properties.

The TGA curve represents the relationship between temperature and mass loss, allowing for the identification of decomposition temperatures and the quantification of volatile components. The derivative TGA (DTG) curve highlights the rate of weight change, making it easier to detect specific thermal events. In this study, TGA was employed to assess the thermal stability and composition of the composite material. The analysis was performed from 28 °C to 800 °C at a heating rate of 20 °C/min to ensure a comprehensive thermal profile.

7.4 Calculations

7.4.1 Randles-Sevcik equation

The Randles–Sevcik equation describes the relationship between the peak current and the scan rate in cyclic voltammetry. It is commonly used to calculate the diffusion coefficient of electroactive species at planar electrodes. This equation is given by:

$$i_p = 2.69 \times 10^5 \cdot n^{3/2} \cdot A \cdot C \cdot D^{1/2} \cdot v^{1/2} \quad (1)$$

Where:

- i_p is the peak current (A)
- n is the number of electrons transferred in the redox reaction (n=1)
- A is the electrode area (1.13 cm²)
- C is the concentration of the redox species (mol/cm³)
- D is the diffusion coefficient (cm²/s)
- v is the scan rate (V/s)

By measuring i_p at different scan rates and plotting i_p as a function of $v^{1/2}$, the slope of the linear fit can be used to determine the diffusion coefficient using a rearranged form of the equation:

$$D = \left(\frac{Slope}{2.69\times10^5 \cdot n^{3/2} \cdot A \cdot C}\right)^2 \quad (2)$$

7.4.2 *b* values

The *b*-values are key parameters in electrochemical analysis that help differentiate between diffusion-controlled and capacitive-controlled charge storage mechanisms. These values are derived from the relationship between peak current (i_p) and the scan rate (v) in cyclic voltammetry, following the equation 3. (Kim et al., 2020)

$$i_p = av^b \quad (3)$$

where *b* is the *b*-value, which provides insight into the dominant charge storage process. A *b* value close to 0.5 indicates a diffusion-limited process, a characteristic of faradaic intercalation or redox reactions. Conversely, a *b*-value close to 1 suggests a capacitive-controlled process, where charge storage occurs mainly at the electrode surface.

8.- RESULTS

8.1 SEM

Figure 5 presents the SEM analysis of the Si/C composite, providing relevant information about its surface morphology and structural characteristics. The composite generally exhibits a spherical morphology; however, most particles lack a well-defined shape and tend to agglomerate into clusters. This behavior is attributed to the pyrolysis synthesis method used in the process (Gu et al., 2010).

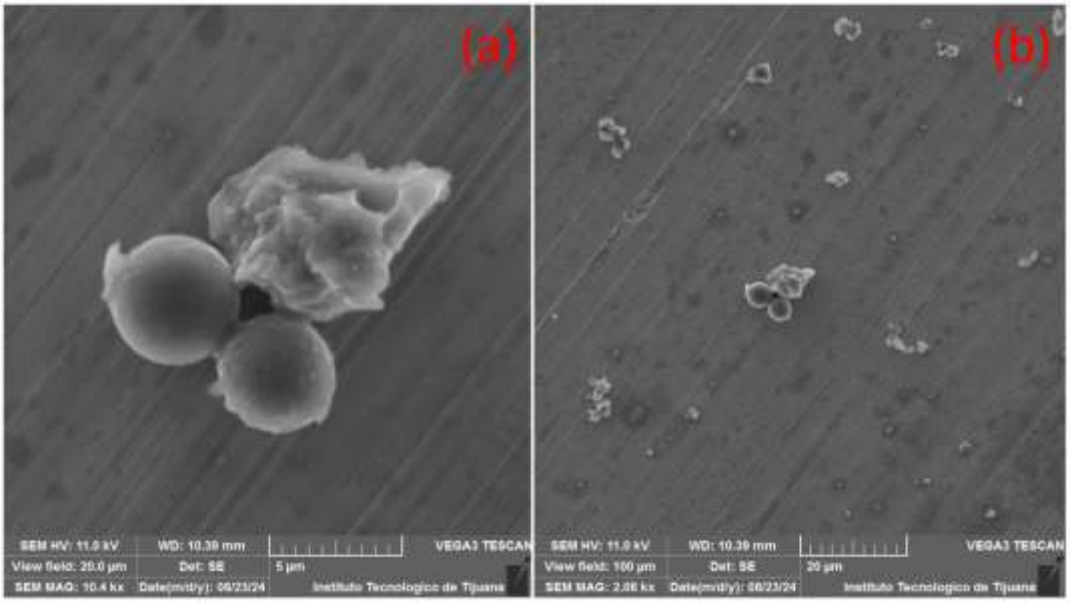

Figure. 5 *SEM image of Si/C composite, a) cluster of the composite Si on a C smooth surface, b) Overview of several clusters of Si at 20 µm.*

The average particle size is 1.97 µm**,** with a standard deviation of 0.89 µm. To further illustrate the particle size distribution, Figure 6 presents a histogram of particle diameter length. This displays a clear view of the sizes of the particles, in which the size distribution curve exhibits a slight Gaussian-like shape, characteristic of a normal distribution, but with a positive skew. This indicates a portion of particles are of larger size within the sample.

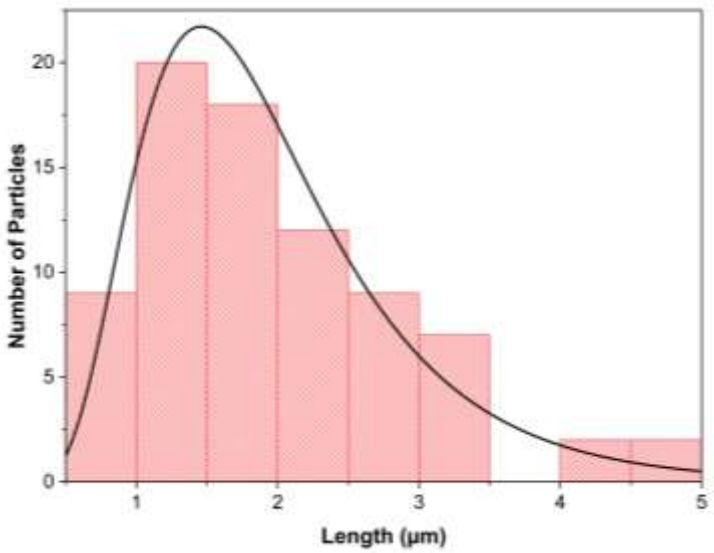

Figure. 6 *Histogram of distribution of size of Si particles.*

8.2 XRD

The XRD study of the composite was conducted to assess the crystallinity state of the material, with the expectation of observing either amorphous characteristics or low crystallinity. The analysis aimed to identify crystalline phases and evaluate the material's structural order. The results, as depicted in Figure 7, provide insights into the phase composition and crystallographic properties of the composite, which are critical for understanding its structural behavior and potential applications.

As can be observed, the presence of the characteristic peak of crystalline silicon at 28.17° (111) confirms the existence of elemental (or pure) silicon. Another high-intensity peak at 26.72° (002) corresponds to graphite, and a broader, lower-intensity peak at 21.05° is attributed to SiO_2 in its cristobalite phase. This latter phase is likely formed during pyrolysis due to PU's and PDMS's oxygen content, which are the synthesized material's precursors.

The three peaks displayed in Figure 7 exhibit low intensity (with the highest peak slightly above 5 a.u.) and considerable broadening, indicating a low degree of crystallinity. This suggests that the material is predominantly disordered, with only small or poorly defined crystalline regions (Li et al., 2007).

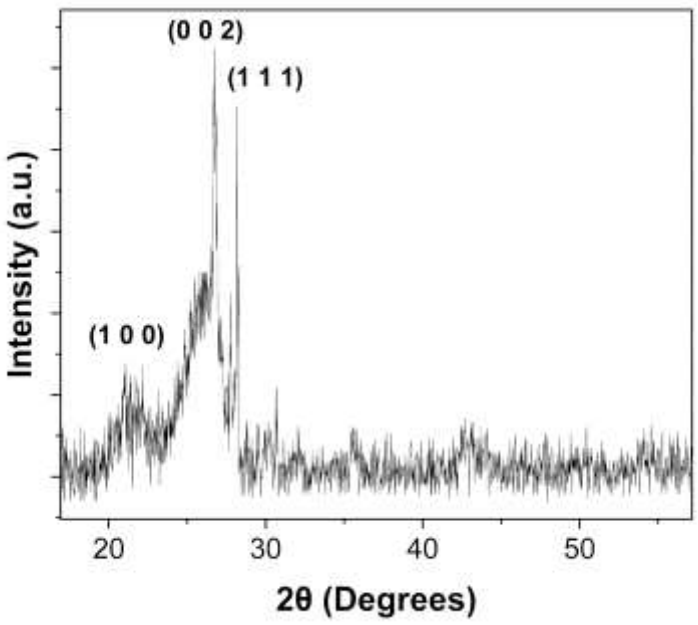

Figure. 7 *XRD analysis of Si/C composite.*

8.3 TGA

The TGA study of the synthesized Si/C composite was conducted to evaluate its thermal stability, decomposition behavior, and composition. By monitoring weight loss as a function of temperature, TGA provides insights into the content of volatile and stable components in the material. At the same time, the residual mass indicates the presence of thermally stable phases. As depicted in Figure 8, the results reveal key details about the material's behavior under thermal stress, including the temperature ranges at which decomposition occurs and the proportion of thermally stable residues. These insights are essential for understanding the material's thermal properties and its potential applications in high-temperature environments.

The TGA curve shows that the Si/C composite begins to lose weight gradually around 460-470 °C, indicating the onset of decomposition or oxidation of residual organic components. A sharp peak in the DTG curve at 550 °C corresponds to rapid decomposition, likely associated with amorphous carbon or remaining organic content. A second, broader peak between 560 °C and 620 °C indicates a slower decomposition process, possibly related to the oxidation of graphitic carbon or minor amounts of silicon oxide (SiO_2). Above 680 °C, the mass stabilizes, confirming the complete removal of volatile and oxidizable components. The final residual mass was 42.18% of the original weight, representing the thermally stable inorganic phases remaining after decomposition. (W. Li et al., 2014)

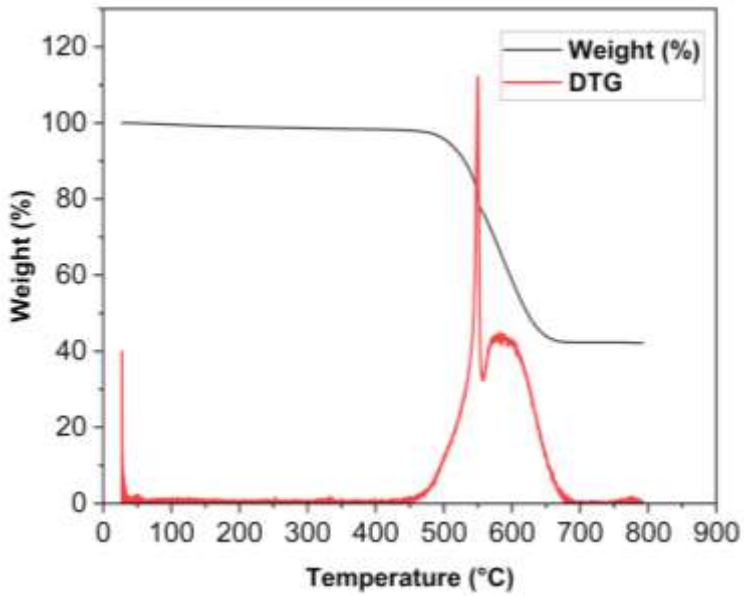

Figure. 8 *TGA and DTG curves of the Si/C composite.*

8.4 Electrochemical evaluation

8.4.1 Cyclic voltammetry (CV)

The cyclic voltammetry (CV) study of the Si/C composite electrode was conducted to evaluate its electrochemical performance and understand its charge storage mechanisms. By analyzing the current response as a function of applied voltage, CV provides critical insights into the redox reactions, capacitive behavior, and kinetic properties of the material. This analysis is essential for assessing the material's suitability as an electrode in energy storage devices, such as lithium-ion batteries.

Cyclic voltammetry (CV) was performed at different scan rates to evaluate the electrochemical behavior of the Si/C composite electrode. As shown in Figure 9, six voltammograms were obtained by applying scan rates of 0.1, 0.2, 0.4, 0.8, 1.6, and 3.6 mV/s. Each graph represents the current response as a function of the applied potential, capturing the charge and discharge processes of the material. The curves demonstrate excellent stability and reproducibility across multiple cycles for each scan rate, indicating consistent electrochemical performance. At lower scan rates (0.1–0.4 mV/s), the voltammograms exhibit well-defined redox peaks, corresponding to specific lithium insertion and extraction reactions. As the scan rate increases, the peaks shift to higher potentials (anodic) and lower potentials (cathodic), reflecting kinetic limitations and changes in the charge transfer dynamics. (Yang & Rogach, 2019)

It can be observed that as the scan rate increases, the stability of the cyclic voltammetry (CV) cycles diminishes, as evidenced in images d, e, and f. At higher scan rates, the electrochemical system struggles to maintain equilibrium, leading to less defined and more distorted voltammograms. Additionally, the precise movement of the redox peaks—both in terms of their horizontal shift (potential) and vertical intensity (current)—becomes less discernible at individual scan rates.

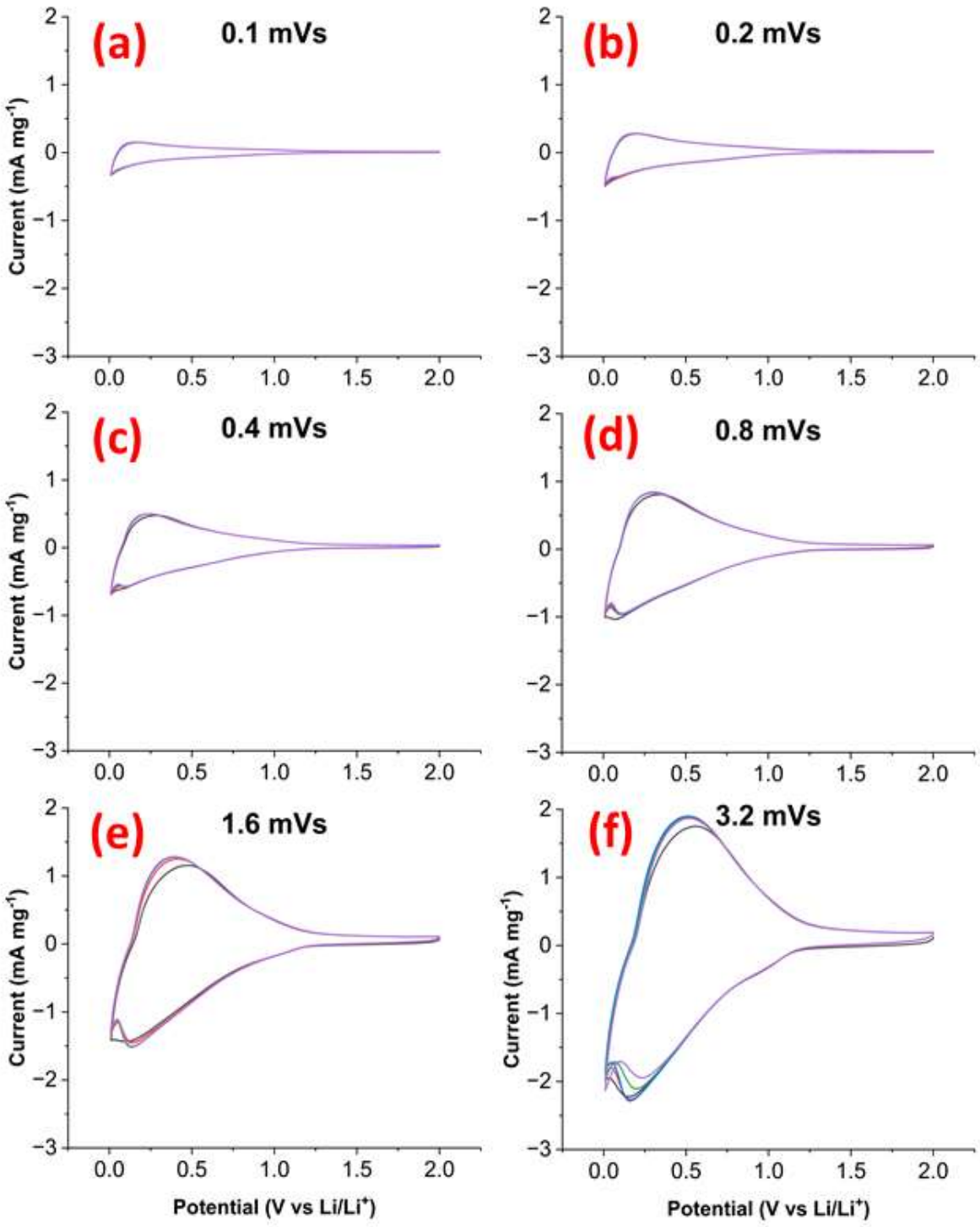

Figure. 9 *Cyclic voltammetry cycles of the Si/C composite electrode at scan rates of (a) 0.1 mV/s, (b) 0.2 mV/s, (c) 0.4 mV/s, (d) 0.8 mV/s, (e) 1.6 mV/s, and (f) 3.6 mV/s.*

Figure 10 presents a consolidated plot of all scan rates overlaid in a single graph to better visualize these trends and analyze the peak behavior. Which reveals significant changes in the electrochemical behavior of the material as the scan rate increases. At

the lowest scan rate (0.1 mV/s), the anodic peak (oxidation) reaches a maximum at 0.15 E/V with a current of 0.15 mA, while the cathodic peak (reduction) is observed at 0 E/V with a current of -0.3 mA. The anodic peaks are broad and elongated, suggesting a gradual oxidation process, while the cathodic peaks are initially less defined but become sharper and more pronounced as the scan rate increases.

Interestingly, at higher scan rates, the cathodic peak exhibits a distinct splitting, forming a small pre-peak followed by a more dominant peak. This behavior is attributed to the lithiation process, where lithium ions are inserted into different sites within the material at slightly different potentials. The appearance of two cathodic features suggests multiple lithiation pathways or a differentiation in the kinetics of lithium insertion, which becomes more pronounced as the scan rate increases.

At the highest scan rate (3.2 mV/s), the anodic peak shifts to 0.5 E/V with a current of 1.9 mA, and the cathodic peak shifts to 0.16 E/V with a current of -2.3 mA. The significant change in peak potentials and the increase in current intensity at higher scan rates reflect kinetic limitations and the dominance of capacitive effects. The anodic peaks (oxidation) shift to higher potentials, while the cathodic peaks (reduction) shift to lower potentials as the scan rate increases. This behavior is consistent with the system's inability to reach electrochemical equilibrium at faster scan rates, requiring higher overpotentials to drive the reactions.

The curves' symmetry is maintained across all scan rates, indicating that the overall electrochemical mechanism remains consistent. However, the broadening of the anodic peaks and the splitting of the cathodic peaks at higher scan rates suggest a transition from diffusion-controlled to kinetically limited behavior. These observations highlight the complex interplay between the material's diffusion, charge transfer, and surface reactions, providing valuable insights into its electrochemical performance and potential application in energy storage devices.

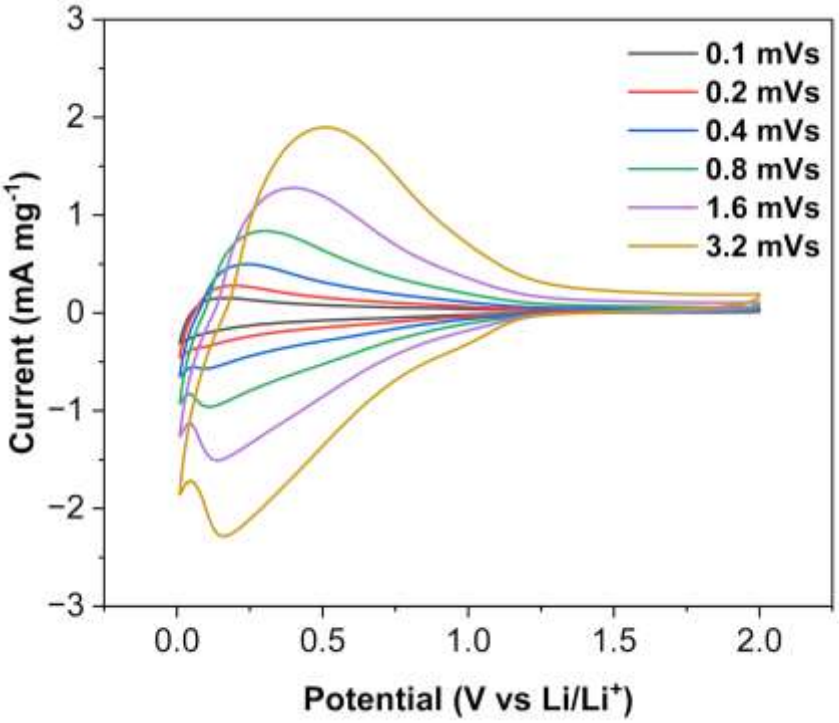

Figure. 10 *Cyclic voltammetry cycles of the Si/C composite electrode at different scan rates comparison.*

8.4.2 Diffusion coefficient (D)

The diffusion coefficient (D) is a fundamental parameter in electrochemical system that describes the rate at which ions move within a material under a concentration gradient. In lithium-ion batteries, D affects charge/discharge rates, energy storage efficiency, and overall battery performance. In this study, D was evaluated to assess lithium-ion mobility within the synthesized Si/C composite electrode and its suitability for energy storage applications. (Ding et al., 2019)

By measuring the peak current (i_p) at different scan rates and plotting i_p as a function of $v^{1/2}$, as shown in Figure 11, the slope of the best-fit line was used to calculate the diffusion coefficient using the Randles–Sevcik equation.

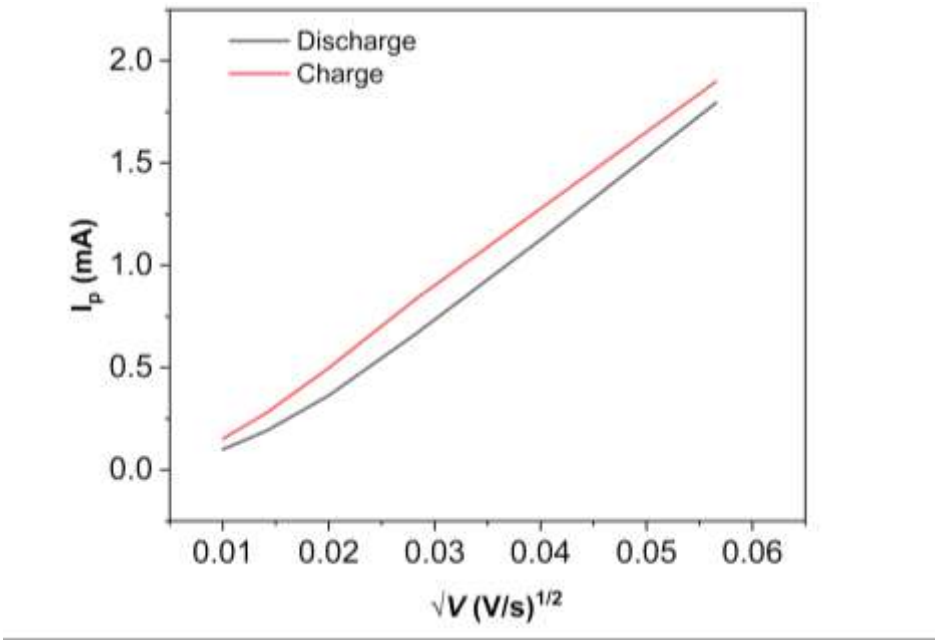

Figure 11. *Plot of the peak current (i_p) versus the square root of the scan rate (v1/2) for the Si/C composite electrode at 25 wt%.*

Table 3. *Diffusion coefficients (D) calculated for the charge and discharge processes*

ELECTRODE	SLOPE		COEFFICIENT	
	Charge	Discharge	Charge	Discharge
SI 25 WT.%	0.03793	0.03695	$1.554 \times 10^{-8} cm^2/s$	$1.4752 \times 10^{-8} cm^2/s$

Table 3 presents the calculated diffusion coefficients for both charge and discharge processes, where the diffusion coefficients obtained for the Si-based electrode with 25 wt.% Si were 1.554×10^{-8} cm²/s during charge and 1.475×10 cm²/s during discharge. The similarity between these values suggests that the lithium-ion transport mechanism remains relatively consistent throughout the intercalation and deintercalation processes. This indicates a good degree of reversibility in the electrochemical reactions. The diffusion coefficients fall within the intermediate range typically reported for silicon-based anode materials, suggesting moderate lithium-ion mobility within the composite structure. When compared to standard diffusion coefficients for conventional graphite anodes (D ≈ $10^{-8\text{-}10}$–10^{-12} cm²/s), the obtained values indicate a significantly higher lithium-ion transport rate, which could contribute to improved rate capability.

8.4.3 *b*-values and contributions

As shown in figure 12, the *b*-values for charge (a) and discharge (b), offer insight into the kinetic behavior of the composite electrode. Reference lines at b = 0.5 and b = 1.0 visually distinguish diffusion- and capacitive-controlled regions. In the charge process (a), the *b*-values initially increase, reaching a peak slightly below 1 before stabilizing around 0.7–0.8, suggesting a mixed charge storage behavior with a significant capacitive contribution. The discharge process (b) shows more stable b-values closer to 0.5, consistent with a diffusion-controlled mechanism. Some scattered points at higher values suggest minor deviations.

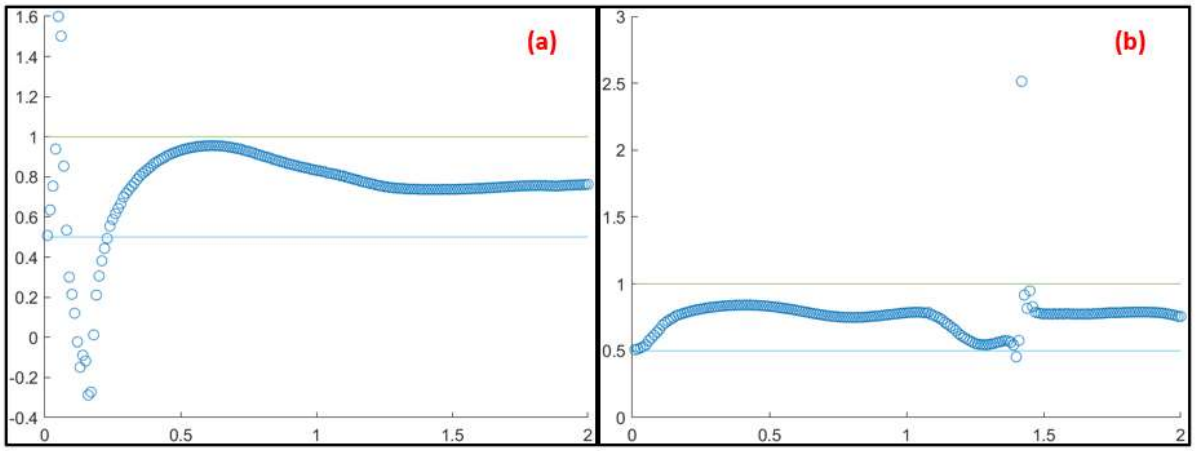

Figure 12. *b-values of Si/C electrode, (a) charge b values, (b) discharge b values.*

To further analyze the charge storage behavior of the electrode, the capacitive and diffusion-controlled contributions were determined as a function of the scan rate. This was achieved by decomposing the CV data into capacitive and diffusion-based currents using computational methods. As shown in Figure 13, the resulting plots provide a quantitative assessment of how these contributions evolve with increasing scan rates, allowing for a more detailed understanding of the electrode's electrochemical performance. (Kim et al., 2020)

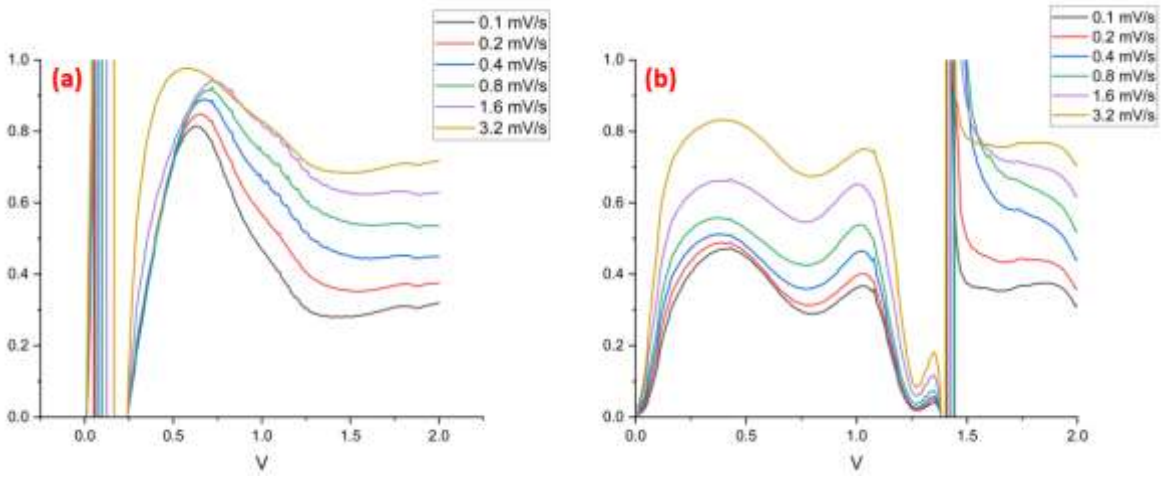

Figure 13. *Capacitive contributions to the total current response of the electrode at different scan rates: (a) charge process and (b) discharge process.*

The capacitive contribution graphs shown in Figure 13 were used to determine the percentage contribution by calculating the area under the curve. This approach allows for a quantitative evaluation of the capacitive effects at different scan rates. The obtained percentage values were then represented in Figure 14, providing a clearer visualization of how the capacitive contribution evolves as a function of scan rate. (Kim et al., 2020)

The capacitive contribution increases with the scan rate for the charge process, starting at 43% at 0.1 mV/s and reaching 78% at 3.2 mV/s. This trend indicates that at higher scan rates, the charge storage mechanism becomes more surface-controlled. Conversely, the diffusion-controlled contribution decreases from 57% to 22% as the scan rate increases, suggesting a reduced influence of diffusion-limited processes at higher rates.

Similarly, for the discharge process, the capacitive contribution follows an increasing trend, rising from 31% at 0.1 mV/s to 66% at 3.2 mV/s. Meanwhile, the diffusion-controlled contribution decreases from 69% to 34%, maintaining a greater diffusion influence compared to the charge process at lower scan rates.

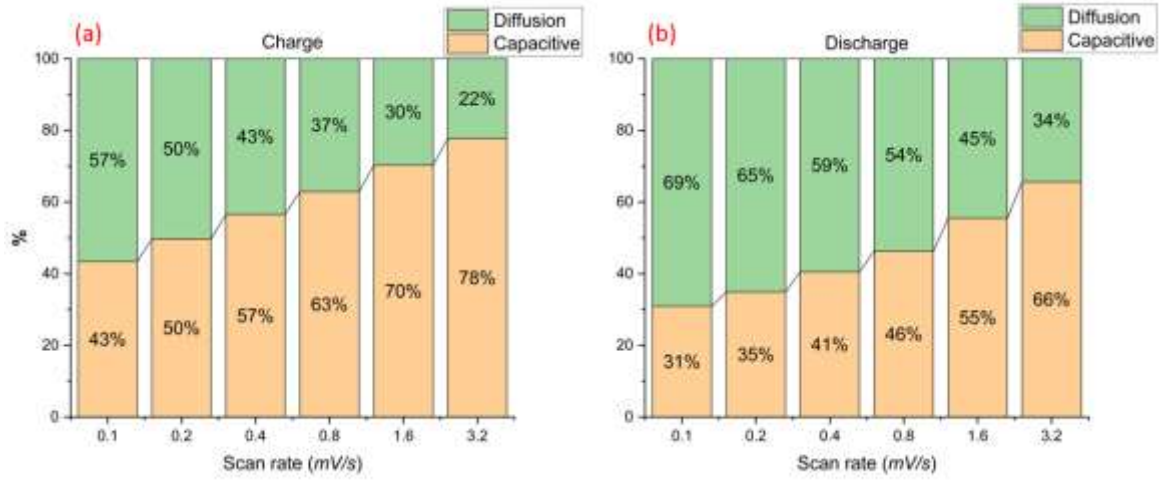

Figure 14. *Capacitive and diffusion contributions for the composite electrode at different scan rates, where (a) corresponds to the charge process and (b) to the discharge process.*

In Figure 15, the distribution of capacitive and diffusion-controlled contributions within the cyclic voltammetry (CV) curve is presented in greater detail. For better visualization, the area corresponding to capacitive effects is highlighted in red, while the area dominated by diffusion-controlled effects is shown in black. This graphical representation provides a clearer interpretation of how each phenomenon contributes to the electrochemical response of the electrode as a function of the scan rate.

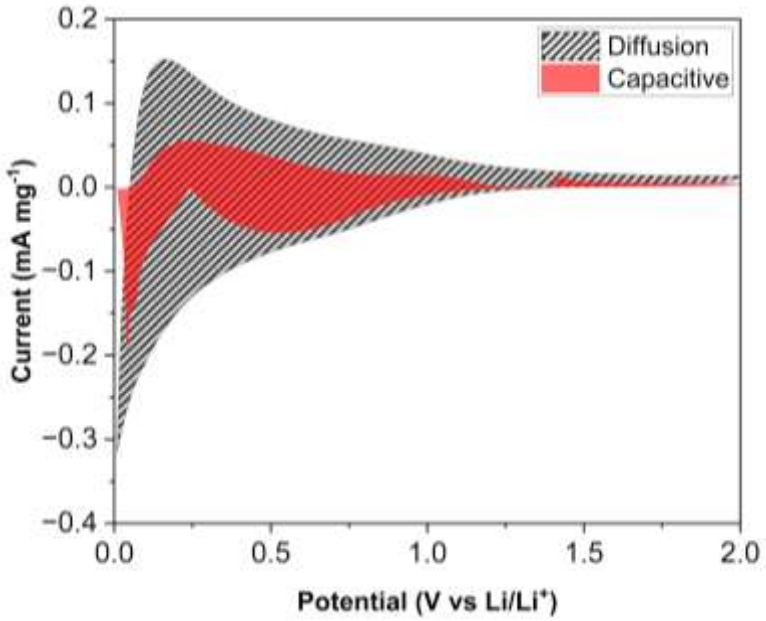

Figure 15. *CV Curve with Faradaic and Non-Faradaic Contributions at 0.1 mV s $^{-1}$.*

9. DISCUSSION

This study evaluated the electrochemical and structural behavior of a Si/C composite at Si 25 wt% using techniques such as XRD, SEM, TGA, CV, and analysis of diffusion and capacitive contributions. The results provide a comprehensive understanding of how silicon distribution within the carbon matrix affects the electrode's stability and performance. The successful synthesis of the material was confirmed, demonstrating favorable outcomes in both its structural properties and electrochemical performance. These findings highlight the composite's potential for advanced energy storage applications.

The synthesis of this composite through pyrolysis is expected to yield an amorphous structure, as confirmed by the XRD analysis. The XRD pattern revealed low-intensity but identifiable peaks corresponding to graphite and silicon oxide (SiO_2), indicating partial crystallinity. While silicon oxide can be detrimental to battery performance by limiting the amount of silicon available for lithium absorption (lithiation), it also provides structural stability to the electrode. This added stability helps mitigate volume expansion during cycling, reducing mechanical degradation and preserving electrode integrity throughout repeated charge-discharge cycles.

The SEM images reveal the distribution of silicon particles within the carbon matrix, as well as their morphology. Most particles display a tendency toward spherical shapes, although some lack defined structure. The images show a relatively uniform distribution of particles across the plane, with slight agglomeration in certain areas. Although agglomeration is not ideal, it does not significantly impair performance due to sufficient overall homogeneity, ensuring effective ion transport and electrochemical activity.

The thermal stability of the material is further confirmed by TGA analysis, which shows the decomposition of carbon starting around 470 °C in a continuous and gradual manner. Although agglomeration is not ideal, it does not significantly impair performance due to sufficient overall homogeneity, ensuring effective ion transport and

electrochemical activity. The final residual mass of 42% corresponds to stable phases of Si and SiO_2.

The electrochemical and kinetic performance of the electrode was evaluated using cyclic voltammetry (CV), which provides comprehensive insights into the material's behavior. The CV curves display stable and reversible electrochemical characteristics without notable distortions. This indicates stable and consistent electrochemical activity, suggesting that the electrode maintains its structural integrity during cycling.

To assess the overall performance of the composite, batteries were assembled using electrodes with different compositions: one made of 100% PU and another of 100% silicone (PDMS). These served as control samples for comparison with the 25 wt% Si/C composite. The 25 wt% Si/C electrode demonstrated superior performance compared to the 100% PU electrode and better stability and shape retention than the 100% Si electrode. As illustrated in Figure 16, the CV curves demonstrate that the Si/C composite has greater stability under electrochemical cycling than either of the control electrodes.

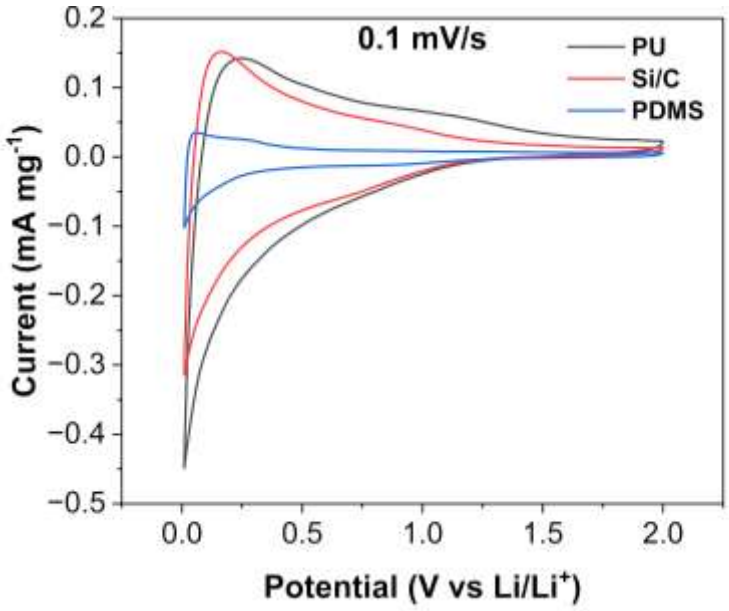

Figure 16. *Cyclic voltammetry (CV) curves of the electrochemical behavior of the Si/C composite (red), 100% PU (black), and 100% PDMS (blue) electrodes at a scan rate of 0.1 mVs-1.*

The diffusion coefficients were calculated using the Randles-Sevcik equation to approximate the kinetic processes within the battery as shown in Table 4. The diffusion coefficients for the charge process were significantly higher than those of the control electrodes, indicating enhanced lithium-ion transport during lithiation. However, during discharge, the diffusion coefficient of the 25 wt% Si/C electrode was only superior to the 100% PDMS control and slightly lower than the 100% PU control. This may be attributed to more efficient delithiation in a pure carbon matrix, where the absence of silicon-lithium bonding facilitates faster ion mobility.

Table 4. *Diffusion coefficients and slopes of i_p vs. $\sqrt{V}$ for the charge and discharge processes of the Si/C composite, PU, and PDMS electrodes.*

ELECTRODE	**SLOPE**		**COEFFICIENT**	
	Charge	Discharge	Charge	Discharge
Si/C	0.03793	0.03695	$1.554 \times 10^{-8} cm^2/s$	$1.4752 \times 10^{-8} cm^2/s$
PU	0.02816	0.04378	$8.569 \times 10^{-9} cm^2/s$	$2.071 \times 10^{-8} cm^2/s$
SI	0.0104	-0.0118	$1.169 \times 10^{-9} cm^2/s$	$1.504 \times 10^{-9} cm^2/s$

Finally, the calculation of the *b*-values is crucial for understanding the dominant processes in the electrode, whether they are electrochemical (diffusion-controlled) or physical (capacitive). As shown in Figure 17, the b-values for the 25 wt% Si/C electrode are close to 0.7, indicating a mixed mechanism with both capacitive and diffusion-controlled contributions. In comparison, the 100% PU control electrode is dominated by diffusion-controlled processes, while the 100% PDMS control electrode exhibits predominantly capacitive behavior due to the nature of the Si material obtained from PDMS pyrolysis. Although XRD indicates the presence of crystalline Si, the formation of amorphous phases or SiOC-like structures may enhance surface-driven lithium storage, increasing capacitive behavior. Additionally, the presence of oxygen and carbon impurities from the pyrolysis process could further modify the electrochemical properties, promoting capacitive behavior.

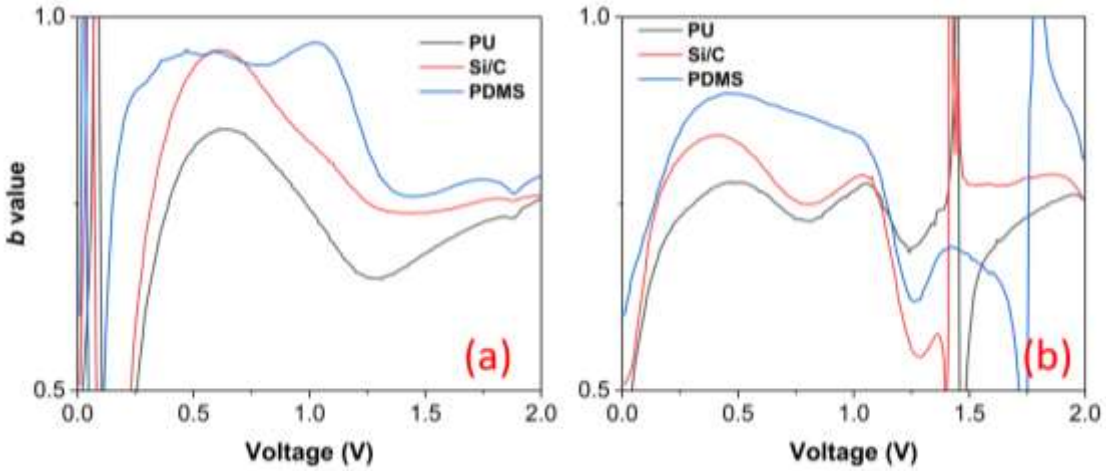

Figure 17. *b values for the PU (black), Si/C composite (red), PDMS (blue) electrodes, indicating the dominant charge storage mechanisms. a) Charge process, b) Discharge process*

This is further reflected in the contribution analysis, where the 25 wt% Si/C electrode shows intermediate capacitive contributions compared to the controls. The higher capacitive contributions in the 25 wt% Si/C electrode can be attributed to surface reactions promoted by the presence of silicon, which are less pronounced in the 100% PU electrode due to the absence of silicon. Although capacitive behavior may reduce total storage capacity by limiting faradaic processes, it also enables rapid charge and discharge, which is advantageous for high-power applications.

10.- CONCLUSION

The Si/C composite electrode, synthesized through the pyrolysis of PU and PDMS, has demonstrated promising electrochemical performance, confirming the success of both the synthesis process and the subsequent characterization. The material shows good capacity retention, cycling stability, and a balanced charge storage mechanism, with a b-value near 0.7, indicating mixed diffusion-controlled and capacitive behavior. Additionally, the Li^+ diffusion coefficients are significantly improved compared to pure silicon, highlighting the beneficial role of the carbon matrix enhancing ion transport kinetics. The electrode also retains its structural integrity after cycling, exhibiting minimal cracking or agglomeration, which underscores its potential for long-term application.

Compared to more complex and high-performance systems reported in the literature, the 25 wt% Si/C electrode holds its own, delivering competitive results in key areas such as capacity, stability, and rate capability. While it may not reach the ultra-high capacities or extreme capacitive dominance of advanced designs, its ease of synthesis and scalability make it a practical, cost-effective option. Moreover, using recycled PU as a precursor aligns with sustainability goals, providing an eco-friendly approach to material development. (Yuan et al., 2025)

Future studies could focus on optimizing the composite further by exploring different weight percentages of silicon and carbon to identify the optimal ratio for enhanced performance. Investigating alternative precursors or refining the synthesis process to remove PU-derived impurities could further improve performance. These efforts would not only improve the electrode's electrochemical properties but also provide deeper insights into the role of each component in the composite. Overall, this work establishes a strong foundation for developing more advanced materials and highlights the viability of recycled PU for sustainable energy storage.

11.- APPENDIX

This section presents the graphs and data used as a reference to compare the performance of the Si/C composite with the control electrodes of 100% PDMS and 100% PU with the values for capacitive and diffusion contributions. These supplementary data allow for a more detailed evaluation of the improvements in the electrochemical performance of the Si/C composite and support the conclusions presented in the main document.

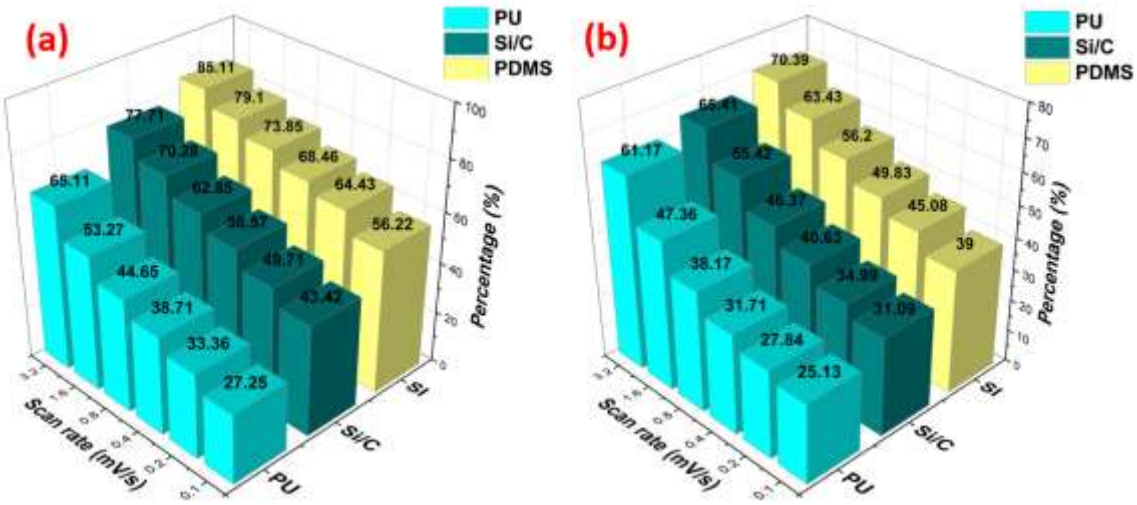

Figure 18. *Three-dimensional bar graph comparing the capacitive contributions (in percentage) of the PU, Si/C composite, and PDMSi electrodes. a) Charge process, b) Discharge process*

12.- REFERENCES

- Arie, A. A., & Lee, J. K. (2010). A study of Li-ion diffusion kinetics in the fullerene-coated Si anodes of lithium ion batteries. Physica Scripta, T139, 014013.
- Baur, J. E. (2007). Diffusion coefficients. En Elsevier eBooks (pp. 829-848). https://doi.org/10.1016/b978-044451958-0.50036-7
- Bryce, E. (2024, March 13). How do chemicals in plastics impact your endocrine system? *Scientific American*. https://www.scientificamerican.com/article/how-do-chemicals-in-plastics-impact-your-endocrine-system/
- De Las Casas, C., & Li, W. (2012). A review of application of carbon nanotubes for lithium ion battery anode material. *Journal of Power Sources*, *208*, 74–85. https://doi.org/10.1016/j.jpowsour.2012.02.013
- Ding, K., Shi, X., Li, C., Gao, X., Han, J., Wang, H., Dou, H., & Pan, J. (2018). Study on the Combustion Products of Dimethyl Silicone Oil as Anode Materials for Lithium Ion Batteries. *International Journal Of Electrochemical Science*, *13*(11), 10859-10872. https://doi.org/10.20964/2018.11.57
- Ding, N., Xu, J., Yao, Y., Wegner, G., Fang, X., Chen, C., & Lieberwirth, I. (2019). Determination of the diffusion coefficient of lithium ions in nano-Si. Solid State Ionics, 180(2-3), 222-225. https://doi.org/10.1016/j.ssi.2008.12.015
- Dubey, R., Rajesh, Y., & More, M. (2015). Synthesis and Characterization of SiO2 Nanoparticles via Sol-gel Method for Industrial Applications. Materials Today Proceedings, 2(4-5), 3575-3579. https://doi.org/10.1016/j.matpr.2015.07.098
- Fafure, A. V., Bem, D. B., Kahuthu, S. W., Adediran, A. A., Bodunrin, M. O., Fabuyide, A. A., & Ajanaku, C. (2024). Advances in Silicon-Carbon Composites Anodes Derived from Agro wastes for Applications in Lithium-ion battery: a review. *Heliyon*, *10*(11), e31482. https://doi.org/10.1016/j.heliyon.2024.e31482
- Gao, S., Yang, D., Pan, Y., Geng, L., Li, S., Li, X., Cao, P., & Yang, H. (2019). From natural material to high-performance silicon based anode: Towards cost-efficient silicon based electrodes in high-performance Li-ion batteries. *Electrochimica Acta*, *327*, 135058. https://doi.org/10.1016/j.electacta.2019.135058

- Gao, W. J., Duan, W. B., Zhang, Y. C., Zhu, J. H., Liu, B., Yang, F. H., & Guo, J. P. (2013). Study of waste rigid polyurethane plastic foam insulation Recycling and Recovery. *Advanced Materials Research*, *743*, 195–198. https://doi.org/10.4028/www.scientific.net/amr.743.195
- Geyer, R., Jambeck, J. R., & Law, K. L. (2017). Production, use, and fate of all plastics ever made. *Science Advances*, *3*(7). https://doi.org/10.1126/sciadv.1700782
- Gu, P., Cai, R., Zhou, Y., & Shao, Z. (2010b). Si/C composite lithium-ion battery anodes synthesized from coarse silicon and citric acid through combined ball milling and thermal pyrolysis. Electrochimica Acta, 55(12), 3876-3883. https://doi.org/10.1016/j.electacta.2010.02.006
- Hu, Q., Tang, Z., Yao, D., Yang, H., Shao, J., & Chen, H. (2020). Thermal behavior, kinetics and gas evolution characteristics for the co-pyrolysis of real-world plastic and tyre wastes. *Journal of Cleaner Production*, *260*, 121102. https://doi.org/10.1016/j.jclepro.2020.121102
- Huang, X., Wang, Z., Knibbe, R., Luo, B., Ahad, S. A., Sun, D., & Wang, L. (2019). Cyclic Voltammetry in Lithium–Sulfur Batteries—Challenges and Opportunities. Energy Technology, 7(8). https://doi.org/10.1002/ente.201801001
- Izarra, I., Borreguero, A., Garrido, I., Rodríguez, J., & Carmona, M. (2021). Comparison of flexible polyurethane foams properties from different polymer polyether polyols. *Polymer Testing*, *100*, 107268. https://doi.org/10.1016/j.polymertesting.2021.107268
- Kang, H. E., Ko, J., Song, S. G., & Yoon, Y. S. (2024). Recent progress in utilizing carbon nanotubes and graphene to relieve volume expansion and increase electrical conductivity of Si-based composite anodes for lithium-ion batteries. *Carbon*, *219*, 118800. https://doi.org/10.1016/j.carbon.2024.118800
- Kim, T., Choi, W., Shin, H., Choi, J., Kim, J. M., Park, M., & Yoon, W. (2020). Applications of Voltammetry in Lithium Ion Battery Research. Journal Of Electrochemical Science And Technology, 11(1), 14-25. https://doi.org/10.33961/jecst.2019.00619
- Larrain, M., Van Passel, S., Thomassen, G., Van Gorp, B., Nhu, T. T., Huysveld, S., Van Geem, K. M., De Meester, S., & Billen, P. (2021). Techno-economic assessment of mechanical recycling of challenging post-consumer

plastic packaging waste. *Resources Conservation and Recycling*, *170*, 105607. https://doi.org/10.1016/j.resconrec.2021.105607

- Li, J., Murphy, E., Winnick, J., & Kohl, P. (2001b). Studies on the cycle life of commercial lithium ion batteries during rapid charge–discharge cycling. *Journal of Power Sources*, *102*(1–2), 294–301. https://doi.org/10.1016/s0378-7753(01)00821-7
- Li, K., Liu, Q., Cheng, H., Hu, M., & Zhang, S. (2020). Classification and carbon structural transformation from anthracite to natural coaly graphite by XRD, Raman spectroscopy, and HRTEM. Spectrochimica Acta Part A Molecular And Biomolecular Spectroscopy, 249, 119286. https://doi.org/10.1016/j.saa.2020.119286
- Li, W., Tang, Y., Kang, W., Zhang, Z., Yang, X., Zhu, Y., Zhang, W., & Lee, C. (2014). Core–Shell Si/C Nanospheres Embedded in Bubble Sheet-like Carbon Film with Enhanced Performance as Lithium Ion Battery Anodes. Small, 11(11), 1345-1351. https://doi.org/10.1002/smll.201402072
- Li, Z., Lu, C., Xia, Z., Zhou, Y., & Luo, Z. (2007). X-ray diffraction patterns of graphite and turbostratic carbon. Carbon, 45(8), 1686-1695. https://doi.org/10.1016/j.carbon.2007.03.038
- Li, Z., Shi, C., Liu, P., Di, Y., Zhang, D., Wang, Q., Sun, H., Sun, Q., & Wang, B. (2024). Homogeneously dispersed silicon/graphite composite toward enhanced lithium-ion batteries. *Journal of Energy Storage*, *88*, 111673. https://doi.org/10.1016/j.est.2024.111673
- Liu, W., Guo, Z., Young, W., Shieh, D., Wu, H., Yang, M., & Wu, N. (2004). Effect of electrode structure on performance of Si anode in Li-ion batteries: Si particle size and conductive additive. Journal Of Power Sources, 140(1), 139-144. https://doi.org/10.1016/j.jpowsour.2004.07.032
- Liu, Y., Hanai, K., Yang, J., Imanishi, N., Hirano, A., & Takeda, Y. (2004). Morphology-stable silicon-based composite for Li-intercalation. Solid State Ionics, 168(1-2), 61-68. https://doi.org/10.1016/j.ssi.2004.01.031
- Malla, P. (s. f.). *Bragg's Law*. Class Twelve Physics.

  https://www.askmattrab.com/notes/1007-Bragg-s-Law

- Saju, S. K., Chattopadhyay, S., Xu, J., Alhashim, S., Pramanik, A., & Ajayan, P. M. (2024). Hard carbon anode for lithium-, sodium-, and potassium-ion

batteries: Advancement and future perspective. *Cell Reports Physical Science*, 101851. https://doi.org/10.1016/j.xcrp.2024.101851

- Sani, H. A., Muhammad, M., Muhammad, A., & Saleh, T. A. (2024). Facile process for recycling the monomers from waste polyurethane with energy recovery. *Next Sustainability*, *3*, 100024. https://doi.org/10.1016/j.nxsust.2024.100024
- Schell, T., Rico, A., & Vighi, M. (2020). Occurrence, fate and fluxes of plastics and microplastics in terrestrial and freshwater ecosystems. In *Reviews of Environmental Contamination and Toxicology* (pp. 1–43). https://doi.org/10.1007/398_2019_40
- Sharma, P., & Vidyarthi, V. K. (2024). Impact of microplastic intake via poultry products: Environmental toxicity and human health. *Journal of Hazardous Materia ls Advances*, *14*, 100426. https://doi.org/10.1016/j.hazadv.2024.100426
- Tian, Z., Wang, Y., Qin, X., Shaislamov, U., Hojamberdiev, M., Zheng, T., Dong, S., Zhang, X., Kong, D., & Zhi, L. (2024). Porous silicon/carbon composites as anodes for high-performance lithium-ion batteries. New Carbon Materials, 39(5), 992-1002. https://doi.org/10.1016/s1872-5805(24)60850-4
- Utekar, S., K, S. V., More, N., & Rao, A. (2021). Comprehensive study of recycling of thermosetting polymer composites – Driving force, challenges and methods. *Composites Part B Engineering*, *207*, 108596. https://doi.org/10.1016/j.compositesb.2020.108596
- Waleed, H. Q., & Fiser, B. (2019). Polyurethane synthesis and classification-A mini-review.
- Wilson, A. M., Way, B. M., Dahn, J. R., & Van Buuren, T. (1995). Nanodispersed silicon in pregraphitic carbons. *Journal Of Applied Physics*, *77*(6), 2363-2369. https://doi.org/10.1063/1.358759
- Wong, R. A., Yokota, Y., & Kim, Y. (2022). Stepping beyond cyclic voltammetry: Obtaining the electronic and structural properties of electrified solid–liquid interfaces. *Current Opinion in Electrochemistry*, *34*, 100964. https://doi.org/10.1016/j.coelec.2022.100964
- Yang, C., Zhang, X., Li, J., Ma, J., Xu, L., Yang, J., Liu, S., Fang, S., Li, Y., Sun, X., Yang, X., Pan, F., Lu, J., & Yu, D. (2020). Holey graphite: A promising anode

material with ultrahigh storage for lithium-ion battery. *Electrochimica Acta*, *346*, 136244. https://doi.org/10.1016/j.electacta.2020.136244

- Yang, L., Li, S., Zhang, Y., Feng, H., Li, J., Zhang, X., Guan, H., Kong, L., & Chen, Z. (2024). Multi-scale design of silicon/carbon composite anode materials for lithium-ion batteries: A review. *Journal of Energy Chemistry*. https://doi.org/10.1016/j.jechem.2024.05.029
- Yang, X., & Rogach, A. L. (2019). Electrochemical Techniques in Battery Research: A Tutorial for Nonelectrochemists. Advanced Energy Materials, 9(25). https://doi.org/10.1002/aenm.201900747
- Yuan, Y., Hu, R., Wang, W., Wang, Y., Zhang, T., & Wang, Z. (2025). Design and fabrication of high-performance multilayer silicon-carbon composite anodes for lithium-ion batteries via femtosecond laser. Journal Of Energy Storage, 110, 115362. https://doi.org/10.1016/j.est.2025.115362
- Zhao, H., Bo, X., Xu, H., Wang, L., Daoud, W. A., & He, X. (2024). Advancing Lithium-Ion Battery Anodes towards a Sustainable Future: Approaches to Achieve High Specific Capacity, Rapid Charging, and Improved Safety. *Energy Storage Materials*, 103696. https://doi.org/10.1016/j.ensm.2024.103696
- Zhao, H., Zuo, H., Wang, J., & Jiao, S. (2024). Practical application of graphite in lithium-ion batteries: Modification, composite, and sustainable recycling. *Journal of Energy Storage*, *98*, 113125. https://doi.org/10.1016/j.est.2024.113125
- Zhou, X., & Liu, Y. (2024). Preparation of Core-shell Si/C/graphene Composite for High-Performance Lithium-ion Battery Anodes. *Synthetic Metals*, 117768. https://doi.org/10.1016/j.synthmet.2024.117768